Article citation info:
Khrulev A, Dmytriev S. Study of pulse jet engine thermodynamic cycle using workflow mathematical modeling. Combustion Engines. 0000;XXX(X):xx-xx. https://doi.org/10.19206/CE-218595

Alexander KHRULEV
Serhii DMYTRIEV

Combustion Engines
Polish Scientific Society of Combustion Engines

Study of pulse jet engine thermodynamic cycle using workflow mathematical modeling

ARTICLE INFO

Received: 23 November 2025
Revised:10 February 2026
Accepted: 25 February 2026
Available online: 16 March 2026

The paper presents a theoretical analysis of possible thermodynamic cycles of a pulse jet engine. To clarify the type of thermodynamic cycle, equations for calculating the polytropic index from instantaneous gas parameters in the combustion chamber are derived. The classic Argus As 014 valved pulse-jet engine workflow, both at static conditions and at 800 km/h, has been simulated. The simulation results confirm the known data that the real operating cycle of a valved pulse jet engine during static conditions is the Lenoir cycle. However, for the engines with straight air intake and with increasing flight speed, the specific workflow nature, i.e. the presence of polytropic pre-compression before heat release, that corresponds to the Humphrey cycle rather than the Lenoir cycle, has been found. Unlike a straight intake engine, a valved pulse jet engine with a side air intake that does not have air pre-compression has also been found to exhibit increased performance with increasing flight speed. The obtained data confirm that, in general, the thermodynamic cycle of a valved pulse jet engine can be represented as the Humphrey cycle, which in specific cases, such as zero flight speed and/or a side air intake, does not experience polytropic pre-compression before heat release and corresponds to the Lenoir cycle.

Key words: *pulse jet engine, pulsejet, thermodynamic cycle, workflow, modeling*

1. Introduction

Although no production pulse jet engines have been developed since World War II, this type of engine has been periodically considered for use in unmanned aerial vehicles (UAV) for 80 years. However, until recently, the generally accepted, long-held concept of limited application of "smart," high-precision, and expensive systems virtually ruled out the need and feasibility of using pulse jet engines in unmanned aircraft. However, the rapidly changing nature of 21st-century military conflicts is forcing a reconsideration of established opinions and proven technologies.

An analysis of some open sources indicates a gradual shift away from expensive, low-production systems, which were just recently considered the only feasible ones for a wide range of operational and tactical tasks [2, 3], toward inexpensive systems for mass production and application [29]. But the first problem arises with the scaling of engine production. Thus, with the number of unmanned aerial vehicles reaching hundreds or even thousands per day, equipping them with piston engines produced in similar series is technically difficult or even economically questionable. Moreover, piston engines are currently not used on UAVs at speeds above 250 km/h [46] and, in principle, do not allow achieving the high flight speeds (700 km/h and above) typical of jet engines. At the same time, mass production of turbojet engines in a series of sizes under consideration is not only extremely difficult technically, but also practically impossible, including for economic reasons. In such a situation, the search for an alternative again naturally leads to the long-forgotten pulse jet engine [32].

However, analyzing any parameters or characteristics of pulse jet engines, with their previous position as "smart" and highly precise, but expensive and unique systems, loses its meaning from the outset. For example, most analysts, when considering a UAV with a pulse jet engine, immediately cite the pulse jet engine's specific fuel consumption [30], which is three times higher than that of a turbojet engine. Further, for added persuasiveness, they usually add the extremely high noise and thermal radiation levels, or even the short service life of the reed valves [21], as well as the "inaccuracy" and "non-selectivity" of German V-1 cruise missiles produced in 1944–45 (as if they were still around this time), after which they lose interest.

In fact, such a superficial analysis is inconsequential. For example, today's UAVs with a range of 1000–1200 km often use 2-stroke piston engines, but no one mentions their specific fuel consumption, which is almost twice that of 4-stroke engines [3]. This example demonstrates that an aircraft's mission performance is determined not by its engine's specific fuel consumption, but by its speed and range. Furthermore, the negative impact of some features of a pulse jet engine, which are important for a single application, is mitigated by mass deployment, where features such as noise and thermal radiation can even become advantages. Moreover, the main advantages of a pulse jet engine for UAV use have remained unchanged for 80 years, particularly in mass-production conditions: extreme simplicity of design, low deployment cost, and scalability without significant capital expenditures. All this makes the use of pulsejets on UAVs of various types, especially high speed, possible, and their research to justify the choice of parameters and their coordination with the characteristics of UAVs relevant.

2. Sources review and problem statement

A preliminary analysis of different sources on pulse jet engine research (Fig. 1) shows that significant progress in developing their theory has not been achieved. Since the late 1940s, there have been virtually no serious experimental studies of the pulse jet engine workflow, except for a few specific problems [1, 43]. As a result, no significant

new data on the processes, parameters, and/or characteristics of aircraft pulsejets, expanding on the known data from the first half of the 1940s from the leading German developers of the classic Argus As 014 engine [9], have been obtained during this entire period.

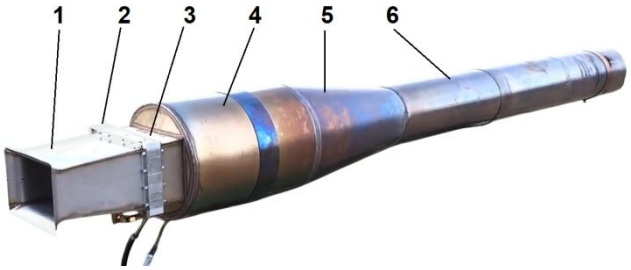

Fig. 1. Schematic diagram of a classic valved pulse jet engine with straight air intake: 1 – inlet device; 2 – valve grid; 3 – Venturi diffuser; 4 – combustion chamber; 5 – cone (nozzle); 6 – resonance tube

The situation with theoretical research is no better. Thus, the method of characteristics [37], developed in the first half of the 1940s, remained, for many decades, one of the few available methods for theoretically studying the pulse-jet engine workflow. Numerous works devoted to theoretical research and the development of methods for modeling motors [8, 44] have not led to greater clarity of the processes than was investigated by the founders of the pulsejet technology in Germany 80 years ago [36]. It is characteristic that even half a century after the creation of this project, in the subsequent decades of general computerization, not a single computer program for modeling the workflow and characteristics of a pulse jet engine has been developed that is accessible to a wide range of users, although significant efforts have been made to this end, including the use of the most modern 3-D modeling [39, 40].

The lack of a systematic approach in research naturally leads to difficulties in assessing the feasibility of various engine designs. As a result, for many decades, numerous enthusiasts, primarily amateurs, unsuccessfully attempted to make various exotic pulsejet designs work, including valveless designs [22, 45], while the experience of German developers clearly indicates the ineffectiveness of such designs in aviation [6] and the practical absence of an alternative to the valve-based pulsejet design [9].

The reasons for these failures are ambiguous. On the one hand, it is worth noting the lack of interest in this engine type in "large" aviation since the late 1940s, which led to the closure of all areas of development and application of aviation pulsejets in favor of turbojet engines. Consequently, research into pulse jet engine processes has become a proactive endeavor, where a lack of, or even complete absence of, adequate funding for this topic prevents the full implementation of all necessary research [35, 38]. On the other hand, significant research has been devoted to investigating pulse combustion [33, 44], including efforts to develop industrial installations and devices based on this phenomenon [26, 27]. Since the purpose of such work was not to obtain the characteristics of an aircraft engine, including thrust and specific fuel consumption, their results have rather limited application for aviation.

In general, it should be noted that the insufficient research into these processes leaves a wide range of possibilities for the emergence of various theories unsupported by theoretical modeling and experiments, which are the basis for numerous attempts to create inefficient [28] or completely inoperable engine designs [41]. This situation is understandable, since for many decades the main field of application of the pulse jet engine was aircraft modeling [11], where the main "scientific centers" were workshops and garages, and the main research tools were metal cutters and welding machines [23]. It is for this reason that significant gaps are observed, first and foremost, in the fundamentals of the theory of pulsejets, including in the study of their thermodynamic cycles.

An analysis of known sources on the topic of pulsejets allows us to draw the preliminary conclusion that German developers clearly justified the thermodynamic cycle of the pulse jet engine as the Lenoir cycle [36]. As is known [34], the ideal Lenoir cycle (Fig. 2a) consists of three processes. Initially, heat is released to the working fluid during isochoric combustion at constant volume, increasing the working fluid's pressure. This is followed by polytropic (adiabatic) expansion, after which heat is released to the environment at constant atmospheric pressure in isobaric cooling. In other words, the key feature of the Lenoir cycle is that pressure increases solely as a result of heat release, without the use of mechanical boosters such as compressors or superchargers. This explains the low maximum cycle pressure, p_{max}, relative to ambient pressure, p_0 – in pulsejets, the cycle pressure ratio ($\pi = p_{max}/p_0$) does not exceed 2.2–2.4.

The closed curve of the component processes forms the diagram of the ideal working cycle (Fig. 2a) of a pulse jet engine. This is not merely a theoretical diagram; on the contrary, it demonstrates that during operation, the state of the working fluid in the engine, not only in the combustion chamber but also in all other sections, undergoes continuous changes in accordance with the circular movement of the diagram at a frequency of 40–200 Hz. This feature characterizes the pulse jet engine as a periodic-flow engine [16], by analogy with an internal combustion engine [4]. But at the same time, it significantly distinguishes this engine from other air-breathing engines (turbojets and ramjets), in which the flow is stationary [42], that is, the state of the working fluid in a specific section of the engine remains constant over time.

Despite the indication of the German developers [36], and also taking into account the fact that no serious theoretical studies of the pulse jet engine cycle have been conducted for almost 80 years, in some sources [7], nevertheless, there have been claims that the engine's workflow is described by another, more efficient thermodynamic cycle – the Humphrey cycle (Fig. 2b).

The main difference between the Humphrey cycle and the Lenoir cycle lies in the preliminary polytropic (adiabatic) compression before the onset of heat release at constant volume [19]. In other words, an engine operating on the Humphrey cycle, unlike the Lenoir cycle, has an additional compression process in the chamber in addition to the combustion itself. In addition, the Humphrey cycle can be

considered a kind of modification of the Brayton cycle, typical of ramjet engines [7], but instead of heat release at constant pressure, heat is released at constant volume, and there is no gas exchange, instead there is a conditional process of heat removal from the cycle to the environment at a constant atmospheric pressure.

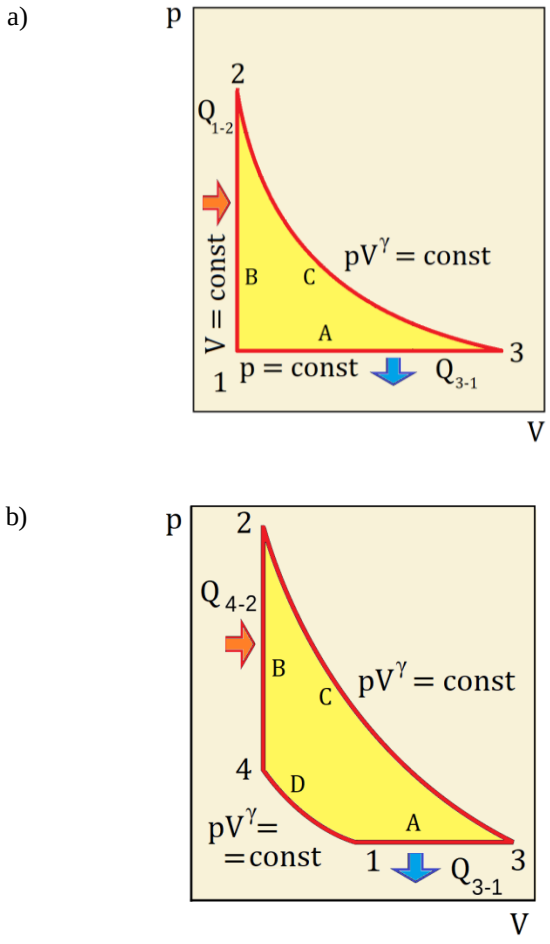

Fig. 2. Diagrams of thermodynamic cycles attributed to a pulse jet engine and their individual processes (phases): a – Lenoir cycle [5], b – Humphrey cycle [7]; A – isobaric gas exchange (intake) and heat removal; B – isochoric heat release (combustion); C – polytropic (adiabatic) expansion; D – preliminary polytropic (adiabatic) compression

According to proponents of this concept [14], preliminary compression also occurs in a pulse jet engine; however, no studies supporting this claim are presented in these works. Some sources provide an additional clarification, albeit without proper justification, stating that the thermodynamic cycle of a pulse jet engine can be represented by two variants [26]. Thus, the cycle of a valve engine when operating at a stationary speed, at zero speed, and a valveless engine remains, as previously believed, the Lenoir cycle [12, 20]. However, at a non-zero flight speed, it was proposed to treat the valve engine cycle as a Humphrey cycle [12]. This later enabled some researchers [7, 14] to completely exclude the Lenoir cycle, treating it as a special case of the Humphrey cycle at zero speed, and to consider the Humphrey cycle as the only working cycle of a pulse jet engine without additional conditions [20]. Thus, contrary to the data of the German founders, it was proposed to describe the working cycle of a pulse jet engine as a modification of a ramjet engine, with heat release at constant volume.

It means adding another process to the Lenoir cycle of a pulse jet engine can create a contradiction. A pulse jet engine, as noted above, is a periodic, not continuous, engine. It features gas exchange, as in an internal combustion engine, rather than constant-temperature heat removal at constant atmospheric pressure, as in other types of jet engines. This workflow characteristic significantly influences seemingly obvious patterns, or at least requires substantiation.

For example, all air jet engine types have an appropriate inlet device that brakes the oncoming airflow, but ramjet and turbojet engines are not engines with a periodic workflow; their operating cycle is open, closed only conditionally by the conventional process of heat removal to the environment at constant atmospheric pressure. In contrast, the pulse jet engine's operating cycle is closed, so the introduction of a new process, such as preliminary braking and air compression, must be substantiated by relevant data.

However, such data is currently unavailable. Furthermore, when describing the pulse jet engine workflow using the Humphrey cycle, well-known designs of valved pulse jet engines [24] with a side intake (Fig. 3) are often omitted. It is perfectly clear that such a design does not allow for straight air intake and pre-compression as flight speed increases. However, the most important fact is that all researchers, without exception, consider only the ideal theoretical cycle of a pulse jet engine. Such a cycle, whether the Lenoir or Humphrey cycle (Fig. 2), bears no relation to specific operating pulsejets constructed of metal. Accordingly, a purely theoretical representation of the workflow, without its connection to real objects and their processes, as well as attempts to use theoretical assumptions without verification and to link them to a specific object of study, do not allow us to identify real operating principles for subsequent practical application.

Fig. 3. McDonnell XPJ40-MD-2 valved pulse jet engine with side air entry (McDonnell TD2D Katydid air target [24])

Therefore, there is every reason to believe that insufficient research into the processes involved has led to uncertainty, or even a contradiction, regarding the actual operating thermodynamic cycle of a heat engine known for over 80 years – namely, the pulse jet engine. It is also unclear which of the known thermodynamic cycles is more efficient in a pulse jet engine, and how to practically implement either cycle in a real product. These questions are quite important, as they may be fundamental both to the correct evaluation of the efficiency of existing pulse jet engine designs and to the development of potential new designs for this type of engine.

In light of the identified contradictions and problems, this work aims to determine the actual operating cycle of a pulse jet engine. To achieve this goal, the following tasks must be resolved:

1) Perform a theoretical analysis of known thermodynamic cycles of a pulse jet engine.

2) Consider the possibility of using software tools to simulate the pulse jet engine cycle.

3) Obtain calculation equations for determining the polytropic exponent in the pulsejet thermodynamic cycle.

4) Simulate the pulse jet engine's workflow, calculate the polytropic exponent, and determine the actual thermodynamic cycle of the pulse jet engine.

5) Compare the obtained thermodynamic cycles of pulsejets of different designs and identify the general effect of flight speed on their workflow.

3. Research materials and methods

3.1. Real operating cycle of pulse jet engine: preliminary notices

At first, a valved pulse jet engine operating under static conditions, that is, at zero airspeed, has been considered. Next, analyze the operating cycle of such an engine, taking into account that, as reported in various sources [19, 31, 36], it corresponds to the Lenoir cycle. We begin with the differences between ideal and real thermodynamic cycles.

In the handbook on internal combustion engine (ICE) theory [10], the relationship between cylinder pressure and its volume in a piston engine, or equivalently, piston position, is commonly referred to as an indicator diagram. This relationship was historically determined using a special indicator device, hence the name of the diagram. Characteristically, an indicator diagram in a piston engine is a graphical representation of the real operating cycle of the internal combustion engine, used to analyze engine efficiency, as opposed to the theoretical (ideal) Otto, Diesel, Atkinson, and Miller cycles, which are typically needed primarily to understand the operating principles of internal combustion engines.

In other words, an indicator diagram is a graphical representation of the change in pressure and volume of gases inside the cylinder during internal combustion engine operation under real conditions. It captures all the features of the real operating cycle, including gas exchange processes, heat loss and combustion imperfections and incompleteness. Obviously, such diagram can be made not only experimentally, on a real engine, but also simulated using an engine computer model through numerical experiments. Thus, the ICE indicator diagram precisely corresponds to the actual operating cycle of a specific engine, from which it was measured experimentally or simulated.

Unlike the ICE, no real operating cycle of a pulse jet engine has been considered to date. Numerous studies only consider theoretical (ideal) Lenoir and/or Humphrey cycles, which are unsuitable for analyzing real engine operation. On the other hand, when analyzing the operating cycle of jet engines with a steady flow of the working fluid [42], it is customary to determine which points correspond to which cross-section of the engine's flow path. This approach to a pulse jet engine yields only the ideal thermodynamic cycle diagram (Fig. 2).

The real operating cycle diagram cannot be constructed in this way; its construction requires certain assumptions, including volumetric combustion (heat release) and a uniform distribution of instantaneous gas parameters throughout the combustion chamber. The key feature of interpreting the real operating cycle of a pulse jet engine is that it lacks a cylinder with a moving piston, and the combustion chamber volume, conventionally defined, remains constant during engine operation. This means that a complete analogy with an ICE is not possible in this case. However, consider the piston analogy or "liquid piston" method [15, 16] adopted when describing gas flow in a resonance tube, the gas volume in a pulse jet engine, limited by the “liquid” piston in the tube, also changes over the cycle time due to gas periodic expulsion. This is generally consistent with the process of an ICE with piston movement in the cylinder.

In ICE theory, it is common to represent the real operating cycle (indicator diagram) in $p - v$ coordinates, where $v = V/m$ is the specific volume of the cylinder, i.e., relative to the mass of gas in the cylinder. This value is the reciprocal of the current (instantaneous) density ρ of the gas in the cylinder, i.e.:

$$v = \frac{V}{m} = \frac{1}{\rho}$$

The same can be achieved in a pulse jet engine. Furthermore, in an ICE, the mass of the gas in the cylinder remains constant during the compression and power strokes, but changes during intake and exhaust (gas exchange). In a pulse jet engine, by contrast, with a constant combustion chamber volume, the mass changes, and the gas exchange process is generally little different from that in an ICE.

In essence, this means that the movement of a hypothetical “liquid” piston in the exhaust tube of a pulse jet engine can be represented by analogy with the movement of a metal piston in an ICE cylinder. In this case, it becomes quite acceptable and reasonable to refer to the real operating cycle diagram of a pulse jet engine as an indicator diagram, as is the case with an ICE. This is indeed important for practice, as it highlights the fundamental difference between the real operating cycle of a pulse jet engine discussed in this paper and the previously widely known ideal theoretical cycle. This name, indicator diagram, for the real operating cycle of a pulse jet engine is proposed in this paper and used below.

3.2. Theoretical analysis of possible thermodynamic cycles of a pulse jet engine

Thus, it is known that the following assumptions are typically made in studies of ideal (reversible) thermodynamic engine cycles [34]:

1) The working fluid is an ideal gas.

2) The mass of the working fluid is constant and the same throughout all processes.

3) Compression and expansion processes are assumed to be adiabatic.

4) Heat is supplied to the working fluid by heat transfer from a hot source.

5) Gas exchange processes are replaced by a reversible process of heat removal from the working fluid to a cold source.

Since such an idealized representation of the workflow is far from reality, it can yield significant errors when used to identify the characteristics of a real engine. For example, assuming a constant mass of the working fluid, an adiabatic expansion process with extremely hot walls, and neglecting the gas exchange processes that determine the filling of the combustion chamber – such crude assumptions make the results of theoretical analysis more than questionable for practical application. It follows that reliable data on the engine's workflow, especially with a periodic one, can only be obtained through the analysis of real cycles. This is confirmed by the experience of theoretical analysis of the operating process of another type of engine with a periodic workflow – internal combustion engines [24].

Indeed, the actual cycle of a pulse jet engine differs significantly from the ideal one, and one of the main differences is that instead of a constant heat removal process at constant atmospheric pressure and a constant mass of the working fluid, the actual cycle involves a process of gas exchange with a variable mass of incoming and outgoing gas. It is also known that during this period, the pressure in the combustion chamber of a pulse jet engine is not constant and does not equal atmospheric pressure, but rather drops significantly to 0.60–0.65 atmospheric [21]. Moreover, in the actual process, one should not expect ideal heat release at constant volume, nor an ideal subsequent adiabatic expansion. All this suggests that the expected indicator diagram of the real cycle (Fig. 4a) will also differ significantly from the ideal one (Fig. 2a). Under such conditions, the polytropic indices of individual processes depicted on the indicator diagram can be particularly important for understanding the operating cycle. To determine patterns of polytropic index change, all possible thermodynamic processes can be represented as functions of their direction (Fig. 4b), with a distinction made between positive (yellow) and negative (blue) polytropic exponent values. Based on these values, the limiting values of the polytropic index can be shown on the real indicator diagram (Fig. 3a).

Thus, approximately halfway through the gas exchange process, the polytropic index increases from –∞ and passes through n = 0, which corresponds to isobaric heat removal (cooling). However, it will continue to increase and, at the beginning of the heat-addition phase, reach +∞. Obviously, during heat addition, a discontinuity in the value of n will occur, since this phase of the process begins at +∞ and ends at –∞, with a transition (discontinuity) from +∞ to –∞. Thereafter, n will gradually increase to approximately the adiabatic expansion exponent γ = 1.4, from where it will gradually increase to +∞, with the new cycle beginning with a discontinuity and again at –∞.

An approximate picture of the change in the polytropic index during a circular walk through the indicator diagram of Fig. 4a is shown in Fig. 5a as a function of time. The cycle is taken to start at the time of intake (gas exchange) at point 3. For comparison, Fig. 5b shows a similar dependence, but for the ideal cycle depicted in Fig. 2a. The vertical line in the middle of the heat addition process indicates a conditional discontinuity associated with the change in sign of the polytropic index from +∞ to –∞ between the end of the isobaric heat removal process with n = 0 and the beginning of the adiabatic expansion with n = γ. The discontinuities in the polytropic index values do not always lend themselves to a precise physical explanation, but in this task, they should be considered and used as transition points between processes.

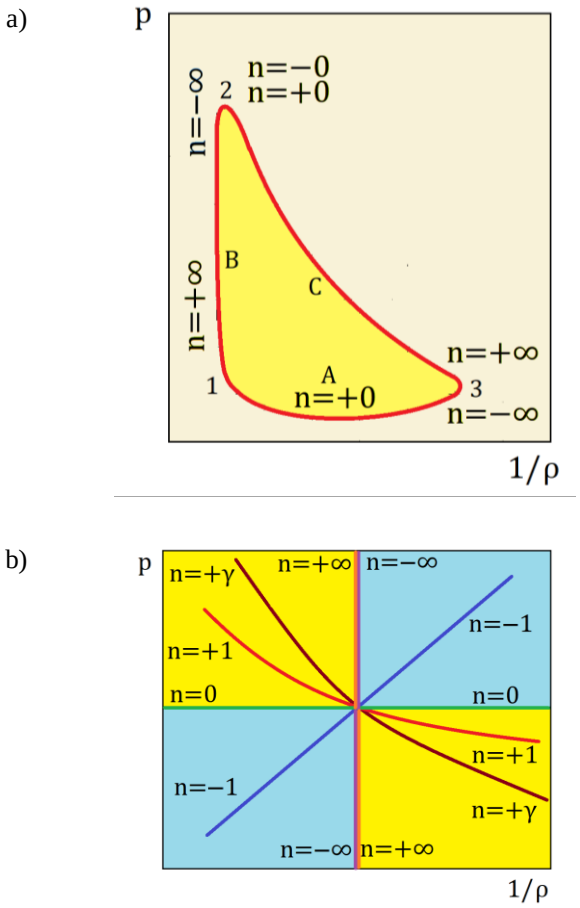

Fig. 4. Changes in the polytropic index in thermodynamic cycles: a – in a hypothetical real operating cycle of a pulse jet engine, constructed based on a theoretical logical analysis of the engine's workflow (the specific volume, the inverse of the gas density, is used instead of volume V); b – ranges of values of the polytropic index of the processes (the field of positive values is shown in yellow, the field of negative values in blue)

Overall, one can note the qualitative agreement between the diagrams of the polytropic index change for the expected real and ideal cycles – despite significant simplifications, the difference in the nature of the n dependence in the ideal cycle (Fig. 5b) and the real cycle (Fig. 5a) is not as great as one might expect.

Similar calculations could be made by assuming that the thermodynamic cycle of a pulse jet engine is a Humphrey cycle. It can then be assumed that at the beginning of the curve's rise, immediately before heat input at constant volume, a section D of polytropic air compression (Fig. 6a) may appear. In this case, a characteristic step will appear in the diagram of the change in the polytropic index (Fig. 6b), corresponding to the transition from the gas-exchange pro-

cess A (3–1) through the preliminary compression D (1–4) to the isochoric heat input B (2–3).

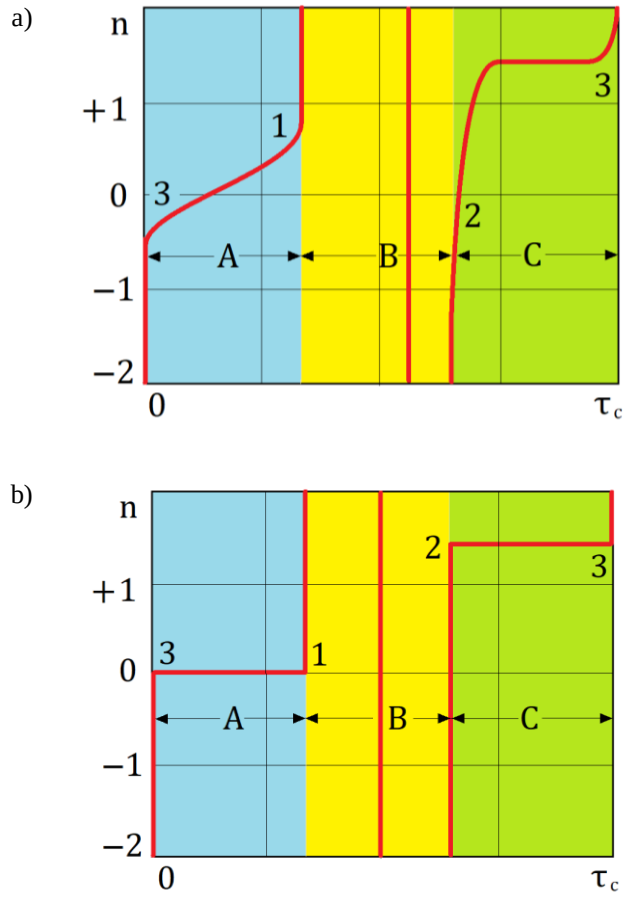

Fig. 5. Change in the polytropic index over time in the operating cycle of a pulse jet engine corresponding to the Lenoir cycle (according to Fig. 2a): a – real cycle (expected change); b – ideal cycle; A – gas exchange (air intake) at constant pressure; B – combustion at constant volume; C – polytropic expansion (exhaust)

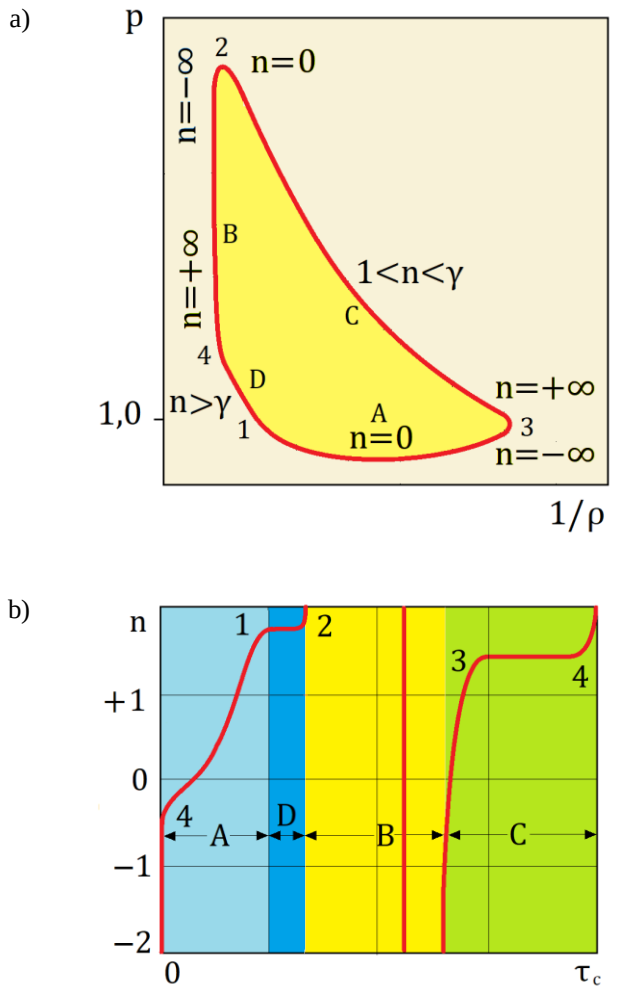

Fig. 6. Representation of the pulse jet engine operating cycle as a thermodynamic Humphrey cycle (according to Fig. 2b): a – hypothetical real cycle; b – hypothetical change in the polytropic index in the real cycle; A – gas exchange (air intake); D – preliminary polytropic compression; B – combustion; C – polytropic expansion (exhaust)

This step should be considered an indication of preliminary compression in the pulsejet working cycle, as shown by a comparison of the nature of the change in the polytropic index for both cycles (Fig. 5b and Fig. 6a). In fact, for the Lenoir cycle (Fig. 5a), there is only a smooth transition of the polytropic index during gas exchange through 0 from –∞ to +∞, while for the Humphrey cycle, after passing through 0, a step must still appear that characterizes the polytropic air compression (braking).

Despite its logical consistency, the theoretical construction of the real operating cycle (Fig. 4–6) may prove erroneous, especially when attempting to accurately depict the aforementioned air deceleration in the inlet device at high flight speeds. Therefore, it is necessary to verify and confirm preliminary assumptions about the actual nature of processes in the real operating cycle.

This can be accomplished by constructing an indicator diagram (and the dependence of the polytropic index change in the cycle) based on modeling the pulse jet engine workflow using the Pulsejet-Sim program [18, 31].

3.3. Using Pulsejet-Sim software for modeling pulse jet engine operating cycle

The Pulsejet-Sim software is based on a thermodynamic model of volumetric combustion of a fuel-air mixture in a combustion chamber and the "piston analogy" model for gas flow in a resonance tube [15]. The program specifies the engine's geometric dimensions and the UAV's flight mode, then numerically calculates changes in the instantaneous gas parameters over time for a selected number of cycles, with increments of 0.01 milliseconds (10^{-5} s).

The calculation results in diagrams of changes in instantaneous pressure and temperature in the combustion chamber, velocity in the resonance tube and intake duct, and other parameters, including an indicator diagram in "pressure-specific volume" coordinates [34]. The program also accounts for air deceleration at the inlet, taking into account total pressure losses (using the total pressure recovery coefficient σ [13]), enabling the comparison of engine operating modes at various flight speeds.

In general, the Pulsejet-Sim program replicates the methods of thermodynamic modeling of instantaneous gas parameters in the cylinder of an internal combustion engine

[17, 25], with the difference that in a pulse jet engine, the combustion chamber volume, unlike in an internal combustion engine cylinder, remains constant [31]. However, both engines share a key property: their workflow is periodic rather than steady-state, making it possible to apply research methods used in internal combustion engines to pulse jet engines.

Thus, by using the program to obtain diagrams of changes in instantaneous gas parameters in the chamber, it becomes possible to calculate the instantaneous value of the polytropic index of the process occurring in the combustion chamber at a given moment.

3.4. Derivation of calculation equations for determining the polytropic index in a pulsejet thermodynamic cycle

To derive the calculation relationships, considered the process of changing gas parameters in the pulsejet combustion chamber. According to the definition of a polytropic process for an ideal gas [34]:

$$pv^n = const \tag{1}$$

where p is the gas pressure; $v = V/m = 1/\rho$ is the gas specific volume; m, V, ρ are the gas mass, volume, and density, respectively.

Let's rewrite equation (1) as:

$$p = \rho^n const \tag{2}$$

Let's assume that the polytropic process occurs between the adjacent time points 1 and 2 in the thermodynamic cycle (the Pulsejet-Sim program calculates 1000 time points during the pulsejet working cycle [18], which yields a very short time interval between time points). Then the following relation holds:

$$\frac{p_2}{p_1} = \left(\frac{\rho_2}{\rho_1}\right)^n \tag{3}$$

Hence, the polytropic index of the process between these points is:

$$n = \frac{\ln\left(\frac{p_2}{p_1}\right)}{\ln\left(\frac{\rho_2}{\rho_1}\right)} \tag{4}$$

From the equation of state of an ideal gas, its density is related to pressure p and temperature T:

$$p = \rho RT \tag{5}$$

where R is the gas constant.

Then equation (4) can be rewritten as:

$$n = \frac{\ln\left(\frac{p_2}{p_1}\right)}{\ln\left(\frac{p_2}{p_1}\frac{T_1}{T_2}\right)} = \frac{\ln\left(\frac{p_2}{p_1}\right)}{\ln\left(\frac{p_2}{p_1}\right) - \ln\left(\frac{T_2}{T_1}\right)} \tag{6}$$

From here, the polytropic index is expressed in terms of the pressure and temperature in the combustion chamber:

$$n = \frac{1}{1 - \frac{\ln\left(\frac{T_2}{T_1}\right)}{\ln\left(\frac{p_2}{p_1}\right)}} \tag{7}$$

For ease of calculations directly from the resulting engine indicator diagram in "pressure-specific volume" coordinates, where the specific volumes are the inverse of the density, expression (4) can be transformed as follows:

$$n = \frac{\ln\left(\frac{p_2}{p_1}\right)}{\ln\left(\frac{\rho_2}{\rho_1}\right)} = \frac{\ln\left(\frac{p_2}{p_1}\right)}{\ln\left(\frac{1/v_2}{1/v_1}\right)} = \frac{\ln\left(\frac{p_2}{p_1}\right)}{\ln\left(\frac{v_1}{v_2}\right)}. \tag{8}$$

Formulas (7) and (8) have a specific points at the beginning of the engine calculation: when the pressures, temperatures, and gas densities in all engine sections are the same and equal to the initial (atmospheric) values, the result of calculations using formula (7) may be undefined and equal to 0/(1–0/0), while using formula (8) it may simply be equal to 0/0.

To eliminate uncertainty, including random uncertainty, a safeguard was introduced into the calculation. Thus, for $p_2/p_1 = 1$, a small value was added to the logarithm in the denominator of the fraction in formula (7):

$$\ln\left(\frac{p_2}{p_1}\right) + 0.00001 \tag{9}$$

A similar technique was used for the entire denominator of formulas (7) and (8).

Thus, when calculating the closed thermodynamic cycle of a pulse jet engine, as determined by its indicator diagram, it becomes possible to obtain a diagram of the change in the instantaneous value of the polytropic exponent throughout the cycle. This diagram can be used to directly determine where and when, in the pulse jet engine cycle (if it occurs at all), the preliminary compression of air during its deceleration in the inlet device occurs, and which thermodynamic process it corresponds to.

4. Research results

The well-known Argus As 014 valved pulse jet engine [9] was selected for the calculations. Even after 80 years, it remains the only fully and comprehensively studied engine of this type [6]. Furthermore, this engine is also one of the standard engines in the Pulsejet-Sim program [18, 31].

After confirming the engine dimensions, the program simulates the start-up and calculates a specified number of cycles (10 cycles were calculated), which allows us to obtain diagrams of instantaneous gas parameters (Fig.7). These parameters are displayed in dimensionless form in the diagrams: pressure p/p_0, temperature T/T_0, gas velocity in the resonance tubev_a/a_0, air velocity at the inlet$v_e/a_0$and heat release rated$Q/dt(1/(a_0Cp_0T_0))$ where parameters with the index "0" correspond to the environment; a_0, Cp_0 are the speed of sound and the heat capacity of the ambient air at constant pressure.

In addition to the diagrams of instantaneous parameters, the program also plots the pulse jet engine's indicator diagram in the "dimensionless pressure – dimensionless specific volume" coordinates for the last specified calculation cycle. To verify the assertion that, at non-zero flight speeds, the thermodynamic cycle of a valved pulse jet engine smoothly transforms from the Lenoir cycle to the Humphrey cycle, similar indicator diagram calculations were also performed for a speed of 800 km/h (Fig. 8). The indicator

diagram data then allows one to directly plot a diagram of the polytropic index change in the pulsejet operating cycle (Fig. 9), using formula (8) for different flight speeds.

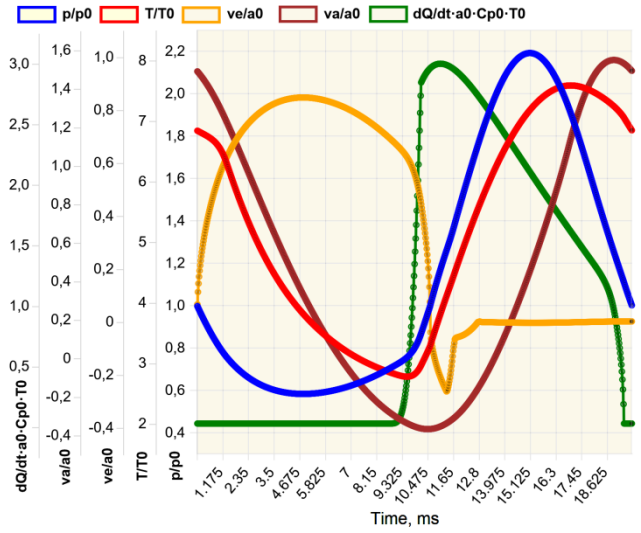

Fig. 7. Diagrams of instantaneous dimensionless parameters: pressure, temperature, inlet velocity, resonance tube velocity, and heat release rate, which were obtained using the Pulsejet-Sim program [31] for the classic Argus As 014 pulse jet engine during operation at zero flight speed $v_f = 0$

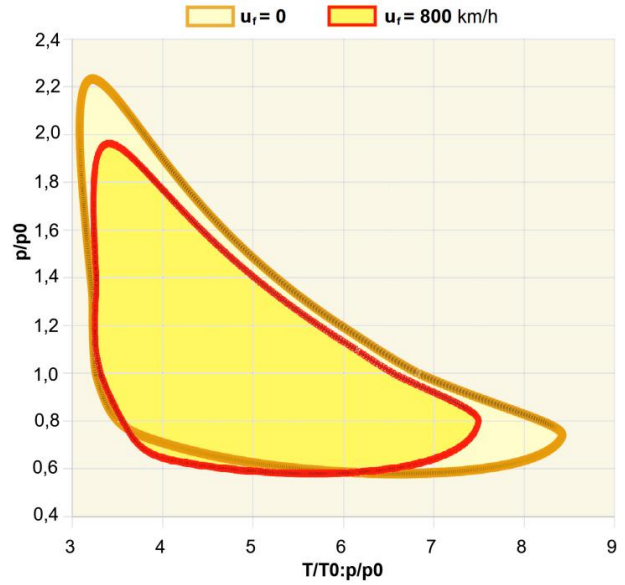

Fig. 8. Indicator diagram (the real operating cycle) of the valved pulse jet engine, obtained using the Pulsejet-Sim program [31] for the Argus As 014 engine during operation at speeds of $u_f = 0$ and $u_f = 800$ km/h

To explain and synchronize the processes, diagrams (from bottom to top) of the heat release rate, inlet air velocity, and combustion chamber temperature and pressure are shown above the diagram of the process's polytropic exponent change. The vertical lines sequentially show four characteristic moments in time (Fig. 9): 1 – the start of combustion (heat release), 2 – reaching the maximum heat release rate, 3 – the end of the intake phase (change in the pressure drop across the valves from positive to negative), and 4 – closing of the valve system petals (end of backflow from the chamber).

In addition, the obtained diagrams of the change in the polytropic index (Fig. 9) conventionally indicate the phases of the pulse jet engine operating cycle, including gas exchange (intake) shown in blue, heat supply during combustion in yellow, and expansion in green.

To ensure a complete study, a simulation of the Argus As 014 engine with a side air inlet was also performed. Fig. 10 presents the operating cycle simulation and calculation results for instantaneous parameter changes, including the indicator diagram and the polytropic index of the process for this engine design at the same flight speed of 800 km/h.

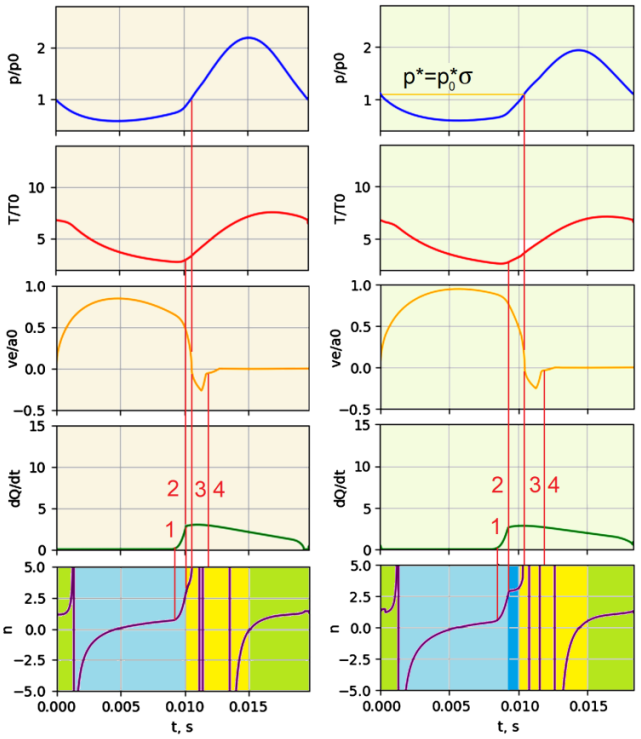

Fig. 9. Calculated change in instantaneous parameters of the Argus As 014 pulse jet engine with parameter synchronization over time in the operating cycle shown in Fig. 7 and 8 (from top to bottom): pressure, temperature, inlet air velocity, heat release rate, polytropic index; a – at zero flight speed $u_f = 0$; b – at flight speed of $u_f = 800$ km/h

5. Discussion and results analysis

From the obtained results, it follows that the calculated indicator diagram (Fig. 8) for static conditions closely matches the diagram constructed solely based on theoretical inferences (Fig. 4a). A fairly close match is also observed between the diagram of the change in polytropic index (Fig. 9a) and the diagram shown in Fig. 4a. This confirms the fact that the thermodynamic cycle of a valved pulse jet engine during stationary operation is a Lenoir cycle. At the same time, as shown in the comparison of the diagrams for a straight intake engine at 0 and 800 km/h (Fig. 9), increasing airspeed and inlet dynamic pressure produce noticeable changes in the indicator diagram.

First, the significant increase in airflow (Fig. 9b) is understandable for a straight intake design with an open downstream resonance tube. However, this design degrades combustion chamber performance at higher airspeeds, as the amplitudes of pressure and temperature fluctuations

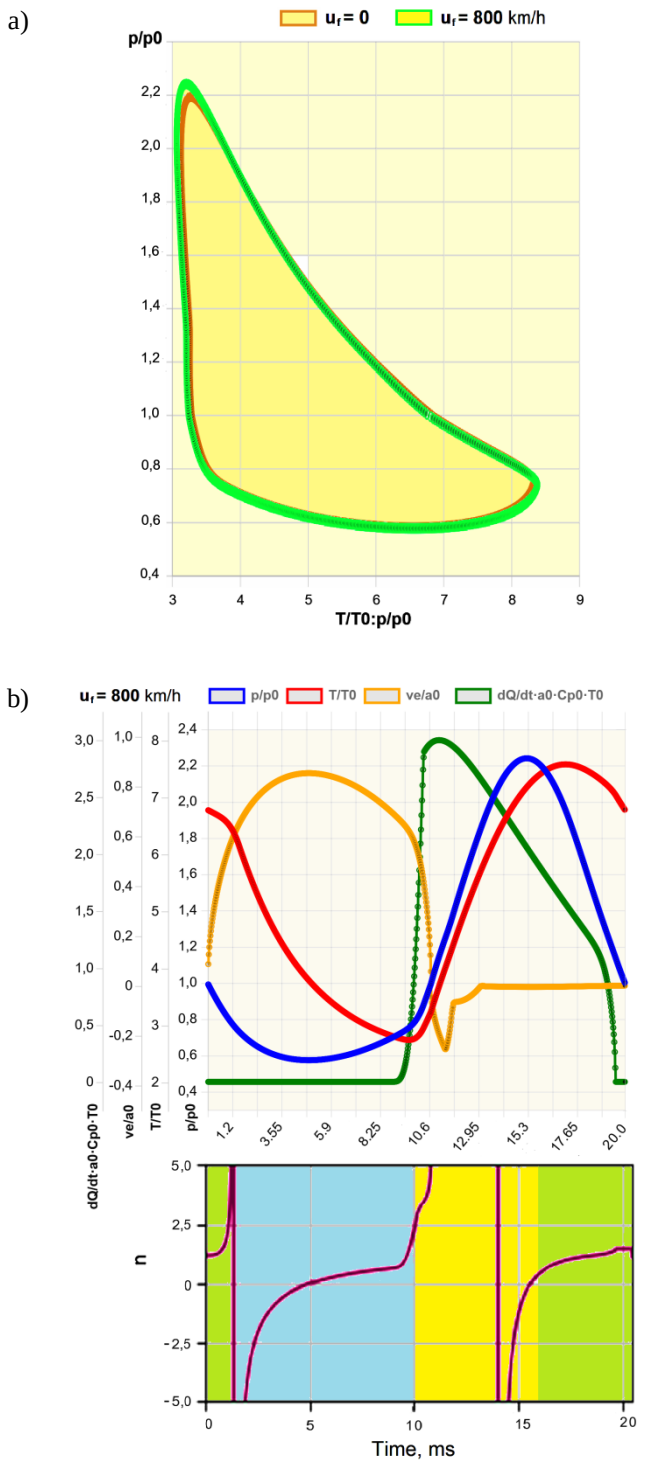

Fig. 10. Results of modeling the workflow of Argus As 014 valved pulse jet engine with a side air intake: a – indicator diagram at flight speeds of 0 and 800 km/h; b – change in instantaneous parameters (top) and polytropic index over cycle time at flight speed of 800 km/h

decrease. This is clearly visible in the indicator diagram (Fig. 8), where, as airspeed increases, a drop in maximum pressure along the vertical axis is accompanied by a proportional drop in maximum specific volume along the horizontal axis, which is proportional to temperature. It's also significant that, as flight speed increases, the air pressure at the engine inlet rises due to the dynamic head (accounting for the total pressure loss). As a result, in the upper diagram at 800 km/h (Fig. 9c), the intake phase begins and ends at a pressure above atmospheric, although below the total free-stream pressure.

The second major difference observed in the indicator diagram of the valved pulse jet engine with a straight air intake at 800 km/h (Fig. 8) is a characteristic slope in the lower-left corner, absent from the indicator diagram for engine operation at zero flight speed. This slope corresponds to a "shelf" in the polytropic index curve at the very beginning of the heat release process (Fig. 9b), which is also absent at zero speed (Fig. 9a).

Let's examine this slope in more detail. As shown in Fig. 9b, at the end of the gas exchange (intake) process, the polytropic index stabilizes for some time at $n > 2.5$, which is significantly higher than in the adiabatic process with $n = \gamma$. In other words, this is a polytropic pre-compression process, but with a significant energy loss.

Such losses are understandable. Really, in a valved engine, significant hydraulic losses should be expected as air flows through the petal valve grid. Furthermore, the Pulsejet-Sim program calculates instantaneous pressure and temperature values in the combustion chamber, accounting for heat losses from all outer engine walls, including the resonance tube [18]. Accordingly, heat losses from the combustion chamber during the air inlet process are significant, as indicated by the increased polytropic index. It follows that, as flight speed increases, the actual operating cycle of a valved pulsejet with a straight air intake corresponds to the Humphrey cycle, not the Lenoir cycle.

However, the validity of this statement for all valved pulsejets should be verified. Thus, in a valved pulse jet engine with a side air intake, as follows from the diagrams (Fig. 10), the inlet pressure does not increase with increasing flight speed. Accordingly, unlike a straight intake engine (Fig. 8 and 9), a preliminary air deceleration (compression) section does not occur in a side-entry engine. As a result, the indicator diagram changes only slightly with increasing speed (Fig. 10a). This is confirmed by the appearance of the diagram of the change in the polytropic index for the such engine workflow (Fig. 10b), as well as by its comparison with the diagram of the change in the polytropic index for an engine operating at zero flight speed (Fig. 9a) – in both cases, no air deceleration section is observed.

Therefore, a valved pulse jet engine with a side air intake, unlike a straight intake engine, continues to operate in accordance with the Lenoir thermodynamic cycle even at high flight speeds. However, the results of the study confirm that, at least within the investigated range of parameters and operating conditions, the thermodynamic cycle of a valved pulse jet engine can be represented as a Humphrey cycle, which in special cases, at zero flight speed and/or with a side air intake, does not have polytropic pre-compression before the heat supply and corresponds to the Lenoir cycle.

Significantly, a comparison of the pulsejet cycles of different designs (Fig.8 and 10a) at zero flight speed and high-speed flight indicates a clear advantage of the side-intake engine operating on the Lenoir cycle over the classic straight intake pulse jet engine operating on the Humphrey

cycle. At least, the cycle work, estimated by the area under the indicator diagram curve, at high flight speed, is significantly higher for the side-inlet engine operating on the Lenoir cycle. However, due to limitations in the parameter ranges and operating modes considered, as well as the assumptions and errors of the methods used, the results obtained are preliminary and require further study, verification, and justification (or refutation).

6. Conclusions

A preliminary theoretical analysis of possible thermodynamic cycles of a pulse jet engine revealed that two types of thermodynamic cycles – the Lenoir cycle and the Humphrey cycle can correspond to the workflow of this type of engine. At the same time, a significant difference between the theoretical ideal cycle of a pulse-jet engine and its actual operating cycle is noted. The characteristics of the real operating cycle and the similarity of its processes to those of internal combustion engines suggest that it can be called the indicator diagram of a pulse jet engine.

To clarify the type of thermodynamic cycle of a pulse jet engine, equations for calculating the polytropic index based on instantaneous values of gas parameters in the combustion chamber, were derived. The classic Argus As 014 valved pulse jet engine workflow was simulated using the Pulsejet-Sim program at both static condition and at a flight speed of 800 km/h.

The workflow simulation results show that the actual thermodynamic cycle of a valved pulse jet engine in static condition is the Lenoir cycle. However, in a straight intake engine, the shape of the indicator diagram changes with increasing flight speed, developing a characteristic slope absent at zero flight speed. At the same time, the polytropic index curve before the onset of heat release exhibits a brief stabilization at $n > 2.5$, which is significantly higher than in an adiabatic process with $n = \gamma$ and corresponds to a polytropic pre-compression process. This process pattern indicates significant hydraulic and heat losses from the combustion chamber during the air intake process, but confirms that the real thermodynamic cycle of a straight intake valved pulse jet engine at high flight speed corresponds to the Humphrey cycle, not the Lenoir cycle.

Unlike a straight intake engine, in a side-intake valved pulse jet engine, pre-compression of the air does not occur as flight speed increases, and the indicator diagram changes only slightly. As a result, the valved pulse jet engine with a side air intake operates according to the Lenoir thermodynamic cycle across the entire flight speed range.

The study results confirm that, at least within the studied range of parameters and operating conditions, the thermodynamic cycle of a valved pulse jet engine can be represented as a Humphrey cycle. However, in specific cases, such as at zero flight speed and/or with a side air intake, polytropic pre-compression before heat release is absent, and the real operating cycle corresponds to the Lenoir cycle.

Despite the apparent higher efficiency of the Humphrey cycle compared to the Lenoir cycle, due to the design features of the valved pulse jet engine, organizing the workflow at high flight speeds in accordance with the Lenoir cycle (side air intake) may offer advantages in key parameters over the Humphrey cycle (straight air intake). However, this issue requires further research and substantiation.

Bibliography

[1] Anand V, Jodele J, Zakh A, Geller A, Prisell E, Lyrsell O et al. Revisiting the Argus pulsejet engine of V-1 buzz bombs: an experimental investigation of the first mass-produced pressure gain combustion device. Exp Therm Fluid Sci. 2019;109:109910. https://doi.org/10.1016/j.expthermflusci.2019.109910

[2] Austin R. Unmanned Aircraft Systems. UAVs design, development and deployment. Chichester: John Wiley & Sons Ltd 2010.

[3] Beneigh T et. al. Introduction to unmanned aircraft systems. Barnhart RK, Hottman SB, Marshall DM, Shappee E (eds). Boca Raton: CRC Press, Taylor & Francis Group 2012.

[4] Cupiał K, Tutak W, Jamrozik A, Kociszewski A. The accuracy of modeling of the thermal cycle of a compression ignition engine. Combustion Engines. 2011;144(1):37-48.

[5] Dhananiya Lakshmi Sri M, L. Oblisamy L, Mari Prabu G. Combustion of acetylene and its performance in valveless pulse jet engine. International Journal of Engineering Research & Technology. 2016;5(06):135-141. https://doi.org/10.17577/IJERTV5IS060226

[6] Diedrich G. The aero-resonator power plant of the V-l flying bomb. Project SQUID. New Jersey: Princeton 1948. https://apps.dtic.mil/sti/pdfs/ADA800231.pdf

[7] El-Sayed AF. Fundamentals of aircraft and rocket propulsion. London: Springer-Verlag 2016.

[8] Gieras M, Trzeciak AM. New aspects of the pulse combustion process. Energies. 2024;17(6):1427. https://doi.org/10.3390/en17061427

[9] Gosslau F. Development of the V-1 pulse jet. A history of German guided missiles development. Benecke T, Quick AW (eds). First Guided Missiles Seminar. Munich Germany, April 1956. Brunswick. 1957:400-418.

[10] Heywood JB. Internal combustion engine fundamentals. 2nd ed. New York: McGraw-Hill Education 2018.

[11] Home-made Jet Forum. 2025. https://www.pulse-jets.com/phpbb3/index.php

[12] Humphrey cycle. Wikipedia. 2025. https://en.wikipedia.org/wiki/Humphrey_cycle

[13] Kazula S, Wöllner M, Grasselt D, Höschler K. Ideal geometries and potential benefit of variable pitot inlets for subsonic and supersonic business aviation. 8th European Conference for Aeronautics and Space Sciences (EUCASS). 2019: 15. https://doi.org/10.13009/EUCASS2019-314

[14] Khalatov AA, Nemchin AF, Kobzar SG, Kuzmin AV, Borisov II. Pulse detonation engines: current state and results of studies. Part 1: current state. Khalatov AA (ed.). Dnipro LIRA 2024.

[15] Khrulev A. Determination of gas parameters in resonant pipes and channels of engines with a periodic workflow using the piston analogy method. Eastern-European Journal of Enterprise Technologies. 2023;5(7(125)):50-59. https://doi.org/10.15587/1729-4061.2023.288520

[16] Khrulev A, Muntyan V. Mathematical model and computer program development for online modeling of pulse jet engine working cycle, parameters and characteristics. Drone Systems and Applications. 2025;14:1-32. https://doi.org/10.1139/dsa-2025-0027

[17] Khrulev A, Saraiev O, Saraieva I, Vorobiov O. Modeling of thermodynamic processes in internal combustion engine cylinder during cranking in compression measurement tests. Combustion Engines. 2024;198(3):98-109. https://doi.org/10.19206/CE-187380
[18] Khrulev O, Muntyan V. Development of universal mathematical model and computer program for online modeling of valved and valveless pulse jet engines. Aerospace Technic and Technology. 2024;4,2(206):6-29. https://doi.org/10.32620/aktt.2025.4sup2.01
[19] Kumar S, Prasad SS, Krishna V. Design of pulse jet engine for UAV. International Journal of Engineering Research & Technology (IJERT). 2014;3(9):670-675. https://www.ijert.org/research/design-of-pulse-jet-engine-for-uav-IJERTV3IS090544.pdf
[20] Lenoir cycle. Wikipedia. 2025. https://en.wikipedia.org/wiki/Lenoir_cycle
[21] Litke P, Schauer F, Paxson D, Bradley R, Hoke J. Assessment of the performance of a pulsejet and comparison with a pulsed-detonation engine. 43rd AIAA Aerospace Sciences Meeting and Exhibit. 10-13 January 2005, Reno, Nevada. 2005:10. https://doi.org/10.2514/6.2005-228
[22] Lockwood RM. Hiller pulse reactor lift engine. Final report. Advanced research. Report NO. ARD 308. Bureau of Naval Weapons. Propulsion Dept. Contract No. 61-0226-c. Springfield: National Technical Information Service 1963. https://apps.dtic.mil/sti/tr/pdf/AD0601715.pdf
[23] Maddoxjets. The final word in pulsejets. 2025. https://maddoxjets.com
[24] McDonnell PJ40. Wikipedia. 2025. https://en.wikipedia.org/wiki/McDonnell_PJ40
[25] Medina A, Curto-Risso PL, Hernández AC, Guzmán-Vargas L, Angulo-Brown F, Sen AK. Quasi-dimensional simulation of spark ignition engines from thermodynamic optimization to cyclic variability. London: Springer-Verlag 2014.
[26] Melo ASM. Pulsejet engine performance estimation (Versão Revista Após Discussão) Universidade da Beira Interior, Engenharia. Dissertação para obtenção do Grau de Mestre em Engenharia Aeronáutica (Ciclo de estudos integrado). Covilhã: Universidade da Beira Interior 2019.
[27] Meng X, de Jong W, Kudra T. A state-of-the-art review of pulse combustion: principles, modeling, applications and R&D issues. Renew Sustain Energy Rev. 2015;42. https://doi.org/10.1016/j.rser.2015.10.110
[28] Mittal V. The novel pulse jet engine powering the Ukrainian Trembita missile. Forbes: Jan.13;2025. https://www.forbes.com/sites/vikrammittal/2025/01/13/the-novel-pulse-jet-engine-powering-the-ukrainian-trembita-missile/
[29] Newdick T. Pulsejet drone flies, could have big impact on cost of future weapons. The War Zone. Mar 6;2024. https://www.twz.com/news-features/pulsejet-drone-flies-could-have-big-impact-on-cost-of-future-weapons
[30] O'Brien JG. The pulsejet engine – a review of its development potential national technical information service. Springfield: U.S. Department of Commerce. 1974:118. https://apps.dtic.mil/sti/tr/pdf/AD0787439.pdf
[31] Pulsejet engine workflow simulation program Pulsejet-Sim. 2025. https://pulsejet-sim.com/en/
[32] Pulsejet. Wikipedia. 2025. https://en.wikipedia.org/wiki/Pulsejet
[33] Rahmatika AM, Widiyastuti W, Winardi S, Nurtono T, Machmudah S, Kusdianto Joni IM. CFD simulation of pulse combustion's performance. AIP Conference Proceedings. 2016;1712:040006. https://doi.org/10.1063/1.4941883
[34] Rajput RK. Engineering thermodynamics (for engineering students of all Indian Universities and competitive examinations). Third Edition. New Delhi: LAXMI Publications LTD 2007.
[35] Sánchez AA. Design, construction and testing of a Pulsejet engine (versão final após defesa). Dissertação para obtenção do Grau de Mestre em Engenharia Aeronáutica (2º ciclo de estudos). Covilhã: Universidade de Beira Interior 2022.
[36] Schmidt P. On the history of the development of the Schmidtrohr. A history of German guided missiles development. Benecke T, Quick AW (eds). First Guided Missiles Seminar. Munich Germany, April, 1956. Brunswick. 1957: 375-399.
[37] Shultz-Grunow F. Gas-dynamic investigations of the pulse-jet tube. Parts I and II. National Advisory Committee for Aeronautics. Technical Memorandum No. 1131. Technical High School, Aachen, Germany. Washington: NACA 1947: 112.
[38] Szymański GM, Wyrwas B, Klekowicki M, Strugarek K, Nowak M, Ludwiczak A et al. Simulation research of the feasibility of developing a multi-fuel valved pulsejet engine. Combustion Engines. 2025;201(2):91-102. https://doi.org/10.19206/CE-203139
[39] Tao Geng T, Paxson DE, Zheng F, Kuznetsov AV, Roberts WL. Comparison between numerically simulated and experimentally measured flowfield quantities behind a pulsejet. 44th Joint Propulsion Conference and Exhibit, cosponsored by AIAA, ASME, SAE, and ASEE, Hartford: Connecticut, July 21–23. 2008:13. https://ntrs.nasa.gov/api/citations/20080045534/downloads/20080045534.pdf
[40] Tegner J. Analysis of the operation of the pulsejet engine. 33rd Congress of the International Council of the Aeronautical Sciences. Stockholm, Sweden, 4-9 September. Stockholm: 2022:24. https://www.icas.org/icas_archive/ICAS2022/data/papers/ICAS2022_0120_paper.pdf
[41] Tesla pulsejet engine. Texas Tech University. Capstone Design Projects, 2023. https://www.depts.ttu.edu/me/CapstoneDesign_Projects/4-Tesla-Pulse-Jet-Engine.pdf
[42] The jet engines. Fifth ed. Birmingham: Rolls-Royce plc. 1996.
[43] Trzeciak AM, Gieras M. Temperature estimating method for exhaust gases in valveless pulsejet engine. Combustion Engines. 2020;182(3):3-9. https://doi.org/10.19206/CE-2020-301
[44] Van Heerbeek PA. Mathematical modelling of a pulse combustor of the Helmholtz-type. Delft: Delft University of Technology. 2008:146. https://homepage.tudelft.nl/d2b4e/numanal/heerbeek_afst.pdf
[45] Wave Engine Corp. 2025. https://wave-engine.com
[46] Zhang B, Song Z, Zhao F, Liu C. Overview of propulsion systems for unmanned aerial vehicles. Energies. 2022;15: 455. https://doi.org/10.3390/en15020455

Alexander E. Khrulev, DEng. – Senior Researcher, forensic auto expert, International Motor Bureau, Ukraine.
e-mail: *info@engine-expert.com*

Prof. Serhii Oleksiyovych Dmytriev, DEng.– Aircraft Continuing Airworthiness Department, National Aviation University, Ukraine.
e-mail: *sad@nau.edu.ua*